

Critical temperature of thin niobium films on heavily doped silicon

W. M. van Huffelen, T. M. Klapwijk, and E. P. Th. M. Suurmeijer

*Department of Applied Physics and Materials Science Centre, University of Groningen, Nijenborgh 4,
9747 AG Groningen, The Netherlands*

(Received 12 June 1992; revised manuscript received 29 October 1992)

Measurements of the critical temperature are presented for 20–40 nm niobium films on heavily doped *n*- and *p*-type silicon, for a wide range of silicon doping concentrations and sample preparation methods. Contrary to a normal-metal–superconductor bilayer, a depression of the critical temperature does not occur in the semiconductor–superconductor system. We show the absence of a depression to be consistent with conventional theories for the proximity effect between a superconductor and a normal metal. It is due to the large mismatch in material parameters between the two layers.

I. INTRODUCTION

In the past few years, interest in semiconductor–superconductor structures has increased because of their potential for three-terminal superconducting devices.¹ Although several structures have been realized that carry large supercurrents, a detailed understanding of carrier transport in these structures is lacking. The simplest way to get insight into heterostructures of superconductors (*S*) and semiconductors (*Sm*) is the study of the critical temperature of a *SmS* bilayer. If the semiconductor is degenerately doped it behaves like a normal metal (*N*) and the system can, in principle, be understood as a *NS* bilayer. The easily measured quantity of a *NS* bilayer is the critical temperature T_c^* at which the transition from the normal to the superconducting state occurs. The behavior of T_c^* of a number of superconductor–normal-metal combinations has been studied extensively during the 1960s.^{2–7} Qualitatively, the critical temperature of the superconductor is lowered due to the contact with the normal metal. Most results can be understood in terms of a theory for the superconducting proximity effect developed by de Gennes⁸ and Werthamer and co-workers.^{9,2} Because of the presence of the superconductor, a nonzero superconducting Cooper pair density is found in the normal metal over a characteristic length ξ_N . At the same time the pair density in the superconductor is lowered. The resulting decrease in critical temperature is a measure for the strength of the effect.

An advantage of using a semiconductor instead of a normal metal is the possibility to vary the carrier concentration. The characteristic length ξ_N in the semiconductor depends on the doping concentration, which will affect T_c^* of the bilayer. A disadvantage is that, at the interface of most metal–semiconductor combinations, a potential barrier is present which is doping dependent. The limited transparency for charge carriers of this barrier will diminish the proximity effect and, consequently, the critical temperature reduction of the superconductor. Thus, by studying the critical temperature of superconducting films on a degenerately doped semiconductor, we obtain information about two properties which are gen-

erally relevant for superconductor–semiconductor heterostructures: the penetration depth of Cooper pairs into a semiconductor and the reduction of the number of pairs entering *Sm* due to a barrier at the interface.

In this paper we report on the critical temperature of thin niobium films on a thick, heavily doped, silicon layer. We use films of thickness in the range 20–40 nm, with a critical temperature close to the bulk value.

Contrary to our initial expectations and to results reported by others,¹⁰ niobium films deposited on heavily doped silicon have exactly the same critical temperature as reference films simultaneously deposited on an insulating substrate. This result is verified for an extensive range of film thicknesses, silicon doping, and process parameters. We will show that this null result is consistent with the conventional proximity effect theory for a *NS* bilayer presented in the next section. Its origin is intrinsic and lies in the large difference in diffusion constant and density of states between niobium and silicon.

II. PROXIMITY EFFECT IN A *NS* OR *SmS* BILAYER

A. Normal-metal–superconductor

The critical temperature of a bilayer with superconductor thickness d_S and normal-metal thickness d_N has been obtained by de Gennes for several limiting cases.⁸ The films are assumed to be in the dirty limit [$l \ll \xi$, where l is the elastic-scattering length and ξ the characteristic length defined below (Eq. 3)]. For films with thickness $d > \xi$, de Gennes found the following expression for the critical temperature T_{NS} :

$$T_{NS} = T_{lim} + T_c^0 \left[\frac{2\pi^2 b \xi_S^2 (T_c^0)}{(d_S + b)^3} \right] \exp(-2d_N/\xi_N) \quad (1)$$

with T_{lim} the critical temperature for an infinitely thick normal substrate:

$$T_{lim} = T_c^0 \left[1 - \frac{\pi^2}{2} \frac{\xi_S (T_c^0)^2}{(d_S + b)^2} \right]. \quad (2)$$

In addition to the film thicknesses, the critical tempera-

ture is determined by the quantities b and ξ . The coherence length ξ is given by

$$\xi_{N,S} = \left[\frac{\hbar D_{N,S}}{2\pi k_B T} \right]^{1/2}. \quad (3)$$

In the normal metal, ξ can be interpreted as the penetration depth of Cooper pairs originating from S . Equation (3) represents a diffusion length determined by the characteristic time $\tau = \hbar/2\pi k_B T$.

The so-called extrapolation length b is discussed below. It can be expressed in directly measurable quantities through $b = \rho_N \xi_N / \rho_S$.¹¹

Before focusing on contacts between a semiconductor and a superconductor it is instructive to take a glance at the ‘‘ideal’’ NS interface first, with the only difference between N and S the presence and the absence, respectively, of superconductivity in the isolated material. In this simple case $b = \xi_N = \xi_S$ and the derivative at the interface is given by $d\Delta/dx = \Delta(0)/b = \Delta(0)/\xi_S$ (Fig. 1). Not too far from the critical temperature, the distance p in S over which the order parameter decreases from its bulk value Δ_{bulk} to its interface value $\Delta(0)$ is of the order of $p = a\xi_S$,⁸ with $a \geq 1$. Consequently, the derivative at the interface is also approximately equal to $[\Delta_{\text{bulk}} - \Delta(0)]/a\xi_S$. Equating both derivatives leads to $\Delta(0)/\Delta_{\text{bulk}} = 1/[1+a]$, hence the order parameter at the interface equals at most one-half of the bulk value. We conclude that at the ideal interface the gap is considerably depressed in the superconductor, while b is of the order of the coherence length. As can be seen from Fig. 1, the extrapolation length b presents a measure for the strength of the proximity effect, with a small b implying a strong effect.

B. Semiconductor-superconductor

In principle, the above equations for a NS bilayer can be used to obtain the critical temperature of a SmS bilayer. In doing so, two assumptions are implicitly made which are not *a priori* valid in our system. (1) The theory is based on de Gennes’ boundary conditions which assume a highly transmissive interface. Generally, at a metal-semiconductor interface, a Schottky barrier is present, greatly reducing the interface transmission. As

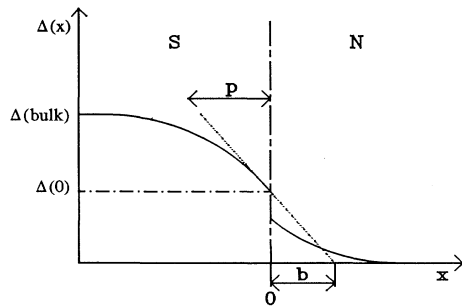


FIG. 1. Behavior of the order parameter $\Delta(x)$ at a NS interface located at $x = 0$. Symbols are explained in the text.

we discuss elsewhere,¹² at the present high doping concentration Schottky barrier theory cannot be applied, but an upper limit to the interface transmission is posed by the large mismatch between the Fermi wave vectors of superconductor and semiconductor. (2) The theory is valid in the dirty limit ($l \ll \xi$). In our samples the semiconductor is not too dirty, l/ξ being on the order of 0.6–0.9. Hence, it is uncertain to which extent the dirty-limit approximation is justified for our samples.

The recent proximity effect theory by Tanaka and Tsukada¹³ does not suffer from these two restrictions. In this theory, reflection and transmission of the wave functions at the interface, due to the difference in Fermi energy between both materials, are explicitly taken into account. The theory is valid near T_c . It connects the dirty and clean ($l \gg \xi$) limits, and can be shown to reproduce the results of de Gennes when $l \ll \xi$ and when the Fermi velocities are equal, both for one- and three-dimensional (3D) systems. The proximity effect is found to be governed by the coefficient σ_{TT} for transmission of Cooper pairs across the interface. The interface transmission decreases when the system becomes cleaner and when the difference between the Fermi velocities becomes larger. The authors report the same expression for the critical temperature lowering as de Gennes [Eq. (1)] with one important modification. The extrapolation length b is replaced by $b_{\text{eff}} = b/\sigma_{TT}$.¹⁴ Interestingly, a very similar result has been obtained previously for the dirty limit,^{15,16} in a straightforward generalization of de Gennes’ theory to include a possible interface barrier. It is demonstrated that de Gennes’ equations for the critical temperature of a bilayer retain their validity if the extrapolation length b is replaced by the effective value $b_{\text{eff}} = b(1+C)$, $C = L_0/\xi_N\sigma$. L_0 is a characteristic length of the order of a mean free path and σ represents the transmission probability of the interface.

We conclude that Eqs. (1)–(3) can be used to predict T_c of a SmS bilayer, provided that the *effective* extrapolation length is used. Additionally, the coherence length in the semiconductor, ξ_{sm} , is obtained by evaluating Eq. (3) in terms of semiconductor parameters. Based on a free-electron model, v_F can be obtained from the carrier concentration n , density-of-states effective mass m_d^* , and value degeneracy ν :

$$v_F = \frac{\hbar}{m_d^*} \left[\frac{3\pi^2 n}{\nu} \right]^{1/3}. \quad (4)$$

The elastic mean free path is determined by the conductivity effective mass m_c^* and the drift mobility μ :

$$l = v_F \tau_{\text{el}} = \frac{m_c^* \mu v_F}{e}. \quad (5)$$

In Eqs. (4) and (5), a distinction is made between effective masses, corresponding to different physical aspects of the semiconductor. The density-of-states effective mass is relevant for calculating the Fermi energy and related quantities, whereas the conductivity effective mass is required for transport phenomena.

Substituting Eqs. (4) and (5) in Eq. (3), the semiconductor length (in the 3D case) is expressed as

$$\xi_{Sm} = \left[\frac{\hbar^3 m_c^* \mu}{6\pi e k T m_d^*} \right]^{1/2} (3\pi^3 n / \nu)^{1/3}. \quad (6)$$

We note that this expression is also useful for theories for the critical current through superconductor-semiconductor-superconductor junctions.¹²

III. SAMPLE PREPARATION AND MEASUREMENTS

For an observable reduction of the critical temperature of a niobium film due to the proximity effect, the thickness d_s should be not too large compared to its coherence length ξ_S . Using $l=5$ nm and $v_F \approx 10^6$ m/s,¹⁷ we estimate $\xi_S = 15$ nm ($T=9$ K). The mean free path l is obtained from the ρl product for niobium,¹⁸ $3.7 \times 10^{-6} \Omega \text{ cm}^2$, and the typical resistivity measured for our niobium films, $\rho = 7.5 \mu\Omega \text{ cm}$. Taking the value for ξ_S as a guideline, we have optimized a process to fabricate good quality niobium films of 20–40 nm thickness still having a critical temperature close to the bulk value of 9.2 K when deposited on an insulator.

Degenerately doped substrates are obtained by implanting boron or phosphorous ions into 1–2.5 $\Omega \text{ cm}$ silicon with (100) and (111) orientation. The implantation doses are 4×10^{14} – $7 \times 10^{15} \text{ cm}^{-2}$ and the implantation energy is 100 keV. After implantation, the wafers are annealed at 950–1100 °C to remove the implantation damage to the silicon crystal, and to activate the implanted ions. A temperature of 900 °C suffices for this. Higher temperatures can be used to obtain a flat doping profile up to a depth of 300–400 nm. A typical doping profile, calculated with the simulation program SUPREMI3 is shown in Fig. 2.

One-half of the area of each silicon wafer is implanted while the other half is left undoped. Nb is deposited on the whole surface, providing a bilayer of Nb on heavily doped Si and a reference Nb film on an insulating substrate in the same run.

Based on previous experiments one expects that a thorough cleaning of the semiconductor substrate before deposition of the superconductor is helpful for the occurrence of a proximity effect.^{19,20} We have varied methods to clean the silicon surface before the Nb deposition. The first steps of these processes are the same. A chemical cleaning is used that grows a protective layer of 1–2-nm silicon dioxide (measured by ellipsometry) on top of the cleaned silicon. After this chemical cleaning, we applied several methods all known from standard silicon technology.

(1) HF dip. Immersing silicon 10–15 s in a 2% HF solution rapidly dissolves the silicon dioxide and subsequently passivates the reactive silicon surface through saturation of the dangling bonds at the surface with H atoms.²¹ The passivation is stable for several minutes longer than the time between the HF dip and loading the sample in the UHV system. Yet, a small amount of hydrocarbons may stick to the surface and about 0.1 monolayer of carbon is usually found.^{21,22}

(2) Shiraki cleaning.²³ The thin and volatile oxide chemically grown on top of the silicon protects its surface

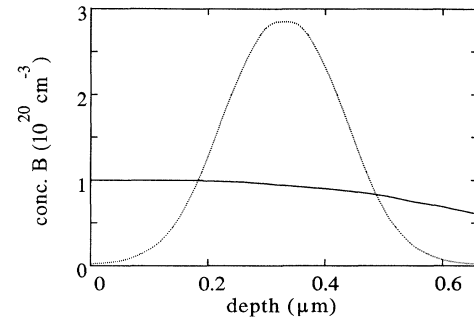


FIG. 2. Doping profile for a $7 \times 10^{15} \text{ cm}^{-2}$, 100-keV boron implantation, calculated with SUPREMI3. Dashed curve: as-implanted profile; solid curve: profile after 30-min anneal at 1000 °C.

during transport. After loading the wafer in a UHV evaporation chamber, the oxide and possible contamination disappear from the silicon surface at temperatures higher than 750 °C. This method produces atomically clean surfaces. We use a 10-min “heatclean” at 820–830 °C. The temperature of the wafer is monitored using a calibrated pyrometer.

(3) Bombardment of the silicon surface with Ar^+ ions. Sputtering the wafer removes contamination from the surface, but it also introduces a certain amount of damage on the surface. Although microscopic details of the surface after sputtering are unknown, this method has been used by several authors^{19,20,24} to fabricate SmS heterostructures. In these cases phenomena attributed to the proximity effect are reported. The present sputter-clean consists of a 4-min bombardment with 1-mA, 600-eV Ar^+ ions originating from a Kaufman source installed in the UHV evaporation chamber.

Based on this variety of cleaning methods we have prepared a series of samples using one of the following steps prior to deposition of niobium.

(I) (a) HF dip. (b) HF dip followed by 10', 830 °C *in situ* heatclean. (c) HF dip followed by an *in situ* sputterclean.

(II) (a) Shiraki cleaning. (b) Shiraki cleaning followed by *in situ* sputterclean at 140 °C.

Wafers cleaned using methods (Ia), (Ib), and (IIa) have also been studied by Auger analysis. After method (Ia), 0.05-ML oxygen and 0.1-ML carbon are found. After method (Ib) only the carbon remains and after method (IIa) less than 0.01 ML of contamination is present. The crystalline quality resulting from method (IIa) has been analyzed by reflection high-energy electron diffraction (RHEED). Perfect 7×7 reconstructions on Si (111) can be observed which are stable for at least 20 h (at a pressure of 10^{-9} mbar), indicating an atomically clean surface. Hence niobium is deposited on a very clean substrate surface.

After chemical cleaning the silicon wafers are brought into an ultrahigh vacuum deposition system with a base pressure of 10^{-10} mbar. Niobium is deposited on the substrate using electron beam evaporation, at a rate of 1.5–2 nm/s and a pressure of 2 – 10×10^{-8} mbar. This background pressure consists of H_2 (>95%) and small amounts of H_2O , CO, CH_3 , and CH_4 ($\leq 2\%$ each). To

prevent water molecules from adsorbing on the substrate it is kept at about 140°C. Immediately after the Nb evaporation a 3-nm silicon “capping” is deposited on top of the Nb, without breaking the vacuum. This procedure is similar to that described by Park and Geballe²⁵ for niobium films on sapphire. The capping prevents oxidation of the Nb film surface when exposed to air. A metallic oxide layer on top of the superconductor could lead to a proximity-effect-induced lowering of T_c . Of course, an intrinsically nonsuperconducting amorphous or polycrystalline silicon layer is present on the niobium. Since this silicon is undoped it is an insulator at low temperatures and no proximity effect should occur between this layer and the Nb film. The thickness of the films is determined from a calibrated quartz crystal (accuracy of 3–5 %).

After Nb deposition the wafers are patterned into a standard Van der Pauw geometry, for a four-terminal measurement of the resistivity ρ . The resistance of the samples is measured using standard lock-in techniques, employing a small ac excitation of usually 1 μ A. We have verified that the measuring current has no effect on the value of the critical temperature by varying it from 50 nA up to 50 μ A. The critical temperature is defined as the temperature at which the resistance of the sample equals one-half of the value at 10 K. To measure the critical temperature, the samples are mounted on a copper block placed inside a vacuum can immersed in liquid helium. The tapered grease seal of the vacuum can is based on a design described by Swartz.²⁶ A calibrated germanium thermometer is thermally anchored to the copper block, as is a heating resistor. The copper block is thermally connected to the helium bath through a changeable thermal resistor. This setup was developed to provide good temperature control between 1.5 and 20 K. The absolute value of the measured temperatures is known within 0.03 K, for relative measurements the accuracy is 0.01 K.

In Fig. 3, a few points of the resistive transition of a 30-nm niobium film are shown. Typical values for 30-nm films on insulating substrates are $\rho(10\text{ K}) = 5\text{--}10\mu\Omega\text{ cm}$, $T_c = 8.7\text{--}9.1\text{ K}$. These values indicate high-quality samples. Interfacial NbSi₂ is not formed at the low temperatures used in the fabrication process. At least 500°C is required for silicide formation.^{27,28} The absence of non-

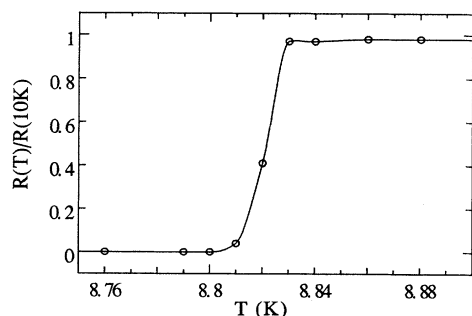


FIG. 3. Transition from the normal to superconducting state, for a 30-nm niobium film with a 3-nm silicon capping, on an insulating substrate. Dots represent the measurement, the solid curve is a guide to the eye.

TABLE I. Critical temperature of thin niobium films on insulating and heavily doped silicon substrates (cleaning methods are explained in the text).

| Doping (10^{19}cm^{-3}) and type | Cleaning method | Thickness (nm) | Resistivity ($\mu\Omega\text{ cm}$) | T_c^* doped (K) | T_c undoped (K) |
|---|--------------------|-------------------|--|-------------------------|-------------------------|
| 1.0 <i>P</i> | IIa | 30.3 | 8.2 | 9.13 | 9.11 |
| 3.0 <i>B</i> | Ib | 20.1 | 8.7 | 8.79 | 8.76 |
| 3.0 <i>B</i> | Ib | 30.0 | 9.3 | 8.99 | 8.96 |
| 3.0 <i>B</i> | IIa | 29.8 | 9.8 | 8.75 | 8.83 |
| 3.0 <i>B</i> | IIa | 39.2 | 6.8 | 9.05 | 9.04 |
| 6.0 <i>P</i> | Ib | 20.4 | 12.2 | 8.75 | 8.71 |
| 6.0 <i>P</i> | Ib | 20.4 | 11.7 | 8.75 | 8.76 |
| 6.0 <i>P</i> | Ib | 30.6 | 9.3 | 9.16 | 9.10 |
| 6.0 <i>P</i> | Ib | 40.7 | 8.1 | 9.05 | 9.11 |
| 6.0 <i>P</i> | IIa | 21.3 | 9.8 | 8.90 | 8.87 |
| 7.0 <i>B</i> | Ia | 30.3 | 9.7 | 8.40 | 8.47 |
| 7.0 <i>B</i> | Ia | 30.3 | 9.8 | 8.47 | 8.46 |
| 7.0 <i>B</i> | Ic | 31 | 6.9 | 8.68 | 8.67 |
| 7.0 <i>B</i> | Ic | 31 | 6.4 | 8.69 | 8.70 |
| 7.0 <i>B</i> | IIa | 30.0 | 5.4 | 8.83 | 8.82 |
| 7.0 <i>B</i> | IIb | 30.1 | 5.9 | 8.89 | 8.89 |
| 10.0 <i>P</i> | Ic | 20.9 | | 8.45 | 8.49 |
| 10.0 <i>P</i> | Ic | 31.2 | 7.0 | 8.83 | 8.89 |

superconducting, metallic surface or interface layers follows from the near-bulk values for T_c : a “dead” layer of 1 nm would already imply a T_c depression of about 1 K.^{25,29} The spread in the critical temperature values for different samples on one wafer is of the order of 0.05 K. The width of the superconducting-normal transition is defined as the difference between the temperatures at which 10 and 90 %, respectively, of the 10-K resistance is reached. This width equals typically 0.01–0.02 K, also illustrating the good quality of the thin films.

An overview of the results accumulated for samples of various film thicknesses, doping concentrations, and cleaning methods is presented in Table I. This table represents our key result. For each set of parameters, films on doped silicon and reference films on undoped silicon have the same critical temperature. The small difference in critical temperature between films on doped and on undoped substrates for a given set of parameters is randomly positive or negative and is of the same magnitude as the variation of the critical temperature over one wafer. Contrary to what one would expect from the analogy with superconducting–normal-metal bilayers, a critical temperature lowering is not observed, independent of silicon doping concentration, carrier type, niobium film thickness, and surface cleaning procedure. Apparently there is an intrinsic difference between NS and SmS systems, inhibiting a substantial decrease of the Cooper pair density in S .

IV. DISCUSSION

Assuming at this point that $b_{\text{eff}} = b$, Eq. (2) can be used to predict the critical temperature reduction of a thin superconducting film on a massive semiconducting substrate. The use of this equation, valid for an infinitely

thick substrate, is justified by comparing the semiconductor coherence length to the depth of the implantation. The latter is at least 300–400 nm (Fig. 3), which is essentially infinite compared to ξ_{Sm} , which equals 8 nm at 9K, for the highest doped substrate. Using typical parameters for our niobium films and the highest doped substrate, $\rho(\text{niobium})=7.5\mu\Omega\text{ cm}$, $\rho(\text{silicon})=550\mu\Omega\text{ cm}$, we find $b=0.6\mu\text{ m}$. The large difference in resistivity between Nb and Si leads to a gigantic value for b . It implies almost no depression of the order parameter takes place in S . Using $\xi_S=15\text{ nm}$ ($T=9\text{ K}$), the reduction of the critical temperature predicted by Eq. (2) for our samples is only 0.01–0.02 K. We conclude that for the limiting case $b_{\text{eff}}=b$ the absence of a depression of the critical temperature in our measurements is consistent with the de Gennes' proximity effect theory for a NS-bilayer.

This conclusion is supported by the extensions of de Gennes' theory^{13,15,16} that are discussed in Sec. II B. These theories lead to the result that the effective extrapolation length b_{eff} is *larger* than b , if the contact is not in the dirty limit, or if the interface transmission is smaller than unity. Thus, the critical temperature shift, which is roughly proportional to $1/b_{\text{eff}}^2$, is even *smaller* than the value predicted by Eq. (2). Physically, reduction of the interface transmission increases the extrapolation length b , indicating a weakened proximity effect (Fig. 1). When the system becomes cleaner, the wave character of the carriers, and consequently, the interface properties, become relatively more important for transport.¹³ This also weakens the proximity effect.

Additional support for the above results is supplied by an advanced treatment of the proximity effect at the NS boundary by Kupriyanov and Lukichev.³⁰ The authors have used the microscopic Eilenberger equations in the immediate vicinity of the interface to find boundary conditions at the SN or SS' interface, valid at any temperature and at any interface transmission. In a recent publication,³¹ it is argued that these general conditions reduce to de Gennes' boundary conditions when the interface transmission is high and the temperature approaches the critical temperature. Within the microscopic framework discussed in Ref. 30 the critical temperature of a bilayer has been obtained only for the limiting case of a bilayer in the dirty limit, with no interface barriers.³² Consequently, the two *a priori* assumptions discussed above cannot be justified by this theory. Nevertheless, it provides an opportunity to compare de Gennes' results to a more advanced approach. As was shown in the numerical example above, according to de Gennes' theory a large difference in normal-state parameters leads to very small critical temperature reductions. From Fig. 4, it is clear that the calculations presented by Golubov *et al.* in Ref. 32 yield essentially the same results. The critical temperature of a NS bilayer is plotted as a function of superconductor thickness for N infinitely thick. Results of de Gennes' theory are also shown. Curves are given for two values of the parameter $\gamma=\rho_S\xi_S/\rho_N\xi_N$; $\gamma=0.02$ correspond to the present niobium-silicon bilayer, whereas $\gamma=1$ represents the ideal NS contact with identical normal-state parameters in N and S . Figure 4 confirms that the critical temperature depression is very small in

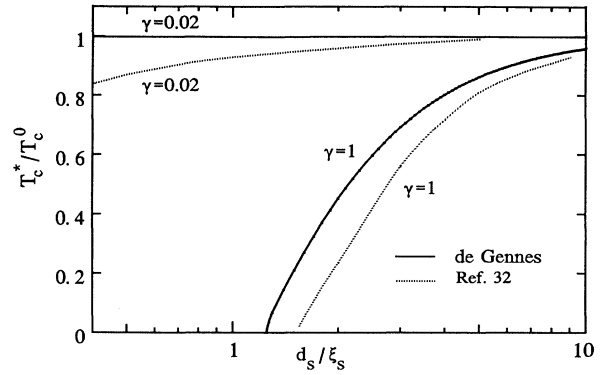


FIG. 4. Critical temperature T_c^* of a NS bilayer, compared to the critical temperature T_c^0 of the isolated superconductor, as a function of the normalized superconductor thickness. The thickness of N is infinite compared to its coherence length. Solid curves: theory of the de Gennes (Ref. 8), dashed curves: theory of Golubov *et al.* (Ref. 32). The parameter γ is defined through $\gamma=\rho_S\xi_S/\rho_N\xi_N$. $\gamma=1$ corresponds to identical normal-state parameters to the Nb-Si bilayers under consideration.

our SmS contact ($d_S/\xi_S\approx 1.3-3$), if Sm is in the dirty limit. It is not clear why the depressions predicted by de Gennes are smaller than Golubov's results. For our films, a critical temperature depression of 0.1–0.6 K is indicated by the latter, but it should be kept in mind that this is calculated for interface transmission equal to unity. A more realistic calculation would probably yield considerably smaller critical temperature shifts.

It is interesting to note that, although the approach of de Gennes and related theories^{13,15,16} is quite different from the approach in Refs. 30–32, a fundamental similarity is present. In both theories, the proximity effect is governed by two parameters:^{33,34} the difference in electronic properties between N and S (expressed by extrapolation length b , respectively, the parameter $\gamma=\rho_S\xi_S/\rho_N\xi_N$, which equals b/ξ_S), and the transmission through the interface (expressed by σ , respectively, a parameter γ_B proportional to the specific boundary resistance). From the general relation $1/\rho=e^2N(E_F)D$, the large difference in resistivity is seen to be equivalent to a large "mismatch" in diffusion constant D and density of states at the Fermi energy, $N(E_F)$.

Our experimental results can only be compared to an experiment by Hatano, Nishino, and Kawabe.¹⁰ They report critical temperature depressions of about 3 K in a 20-nm niobium film on $3\times 10^{19}\text{ cm}^{-3}$ doped silicon. They also find a systematic dependence of T_c^* on the thicknesses of the Nb film and the doped Si layer. We have included their surface cleaning technique [method (Ia), cf. Sec. IV] in our five different methods. We also used up to a factor of 3 higher doping. Nevertheless, we have not found similar critical temperature depressions. Our experimental results are supported by the theoretical analysis presented above, which clearly shows no critical

temperature depression is to be expected in niobium (or other metallic superconductors) on degenerately doped silicon.

V. CONCLUSIONS

We have measured the critical temperature of thin niobium films on degenerately doped silicon for a wide range of silicon doping concentrations, Nb film thicknesses, and different sample preparation methods, for both *n*- and *p*-type silicon. The critical temperature on doped silicon is compared with a reference film on an insulating substrate, prepared simultaneously with the actual sample. Contrary to a superconducting-normal-metal bilayer, a reduction of the critical temperature due to the proximity effect does not take place in the superconductor-semiconductor system. We show the absence of a critical temperature depression to be consistent with the conventional theory for the proximity effect between a normal metal and a superconductor. It is due to the mismatch in material parameters between the two layers. The relevant parameter is $N(E_F)D$, the product of the density of states at the Fermi level and the

diffusion constant. Generally, both are substantially smaller in a semiconductor than in a metal. Physically, the above implies that the depression of the order parameter in *S* is too small to cause a lowering of the critical temperature.

These results are significant for more complex superconductor-semiconductor heterostructures. In these structures, a large mismatch in material parameters between *S* and *Sm* is generally present, leading to an order parameter in *S* that is independent of position. Moreover, an interface barrier is present, which will influence quasiparticle transport and reduce a possible supercurrent.

ACKNOWLEDGMENTS

The authors thank M. Mulder for carrying out the ion implantations and H. Soppe for assistance with the measurements. This research is supported by the Stichting voor Fundamenteel Onderzoek der Materie (FOM), which is part of the Nederlandse Organisatie voor Wetenschappelijk Onderzoek (NWO).

-
- ¹For a review see A. W. Kleinsasser and W. J. Gallagher, in *Modern Superconducting Devices*, edited by D. Rudman and S. Ruggiero (Academic, Boston, 1989); T. M. Klapwijk, D. R. Heslinga, and W. M. van Hutfelen, in *Superconducting Electronics*, edited by H. Weinstock and M. Nisenoff (Springer, Berlin, 1989).
- ²J. J. Hauser, H. C. Theurer, and N. R. Werthamer, *Phys. Rev.* **136**, A637 (1964). In this paper some older experiments concerning NS bilayers are referenced.
- ³P. Hilsch and R. Hilsch, *Z. Phys.* **180**, 10 (1964).
- ⁴J. J. Hauser and H. C. Theurer, *Phys. Lett.* **14**, 270 (1965).
- ⁵G. Bergmann, *Z. Phys.* **187**, 395 (1965).
- ⁶J. J. Hauser, H. C. Theurer, and N. R. Werthamer, *Phys. Rev.* **142**, 118 (1966).
- ⁷A. E. Jacobs and D. M. Ginsberg, *Phys. Rev.* **175**, 569 (1968).
- ⁸P. G. de Gennes, *Rev. Mod. Phys.* **36**, 225 (1964); P. G. de Gennes and E. Guyon, *Phys. Lett.* **3**, 168 (1963).
- ⁹N. R. Werthamer, *Phys. Rev.* **132**, 2440 (1963).
- ¹⁰M. Hatano, T. Nishino, and U. Kawabe, *Appl. Phys. Lett.* **50**, 53 (1987).
- ¹¹W. M. van Hutfelen, Ph. D. thesis, University of Groningen, 1992 (unpublished).
- ¹²W. M. van Hutfelen, T. M. Klapwijk, D. R. Heslinga, M. J. de Boer, and N. van der Post, *Phys. Rev. B* **47**, 5170 (1993).
- ¹³Y. Tanaka and M. Tsukada, *Phys. Rev. B* **37**, 5095 (1988); *Solid State Commun.* **74**, 763 (1990); *Phys. Rev. B* **42**, 2066 (1990).
- ¹⁴In Tanaka and Tsukada's theory, $\xi_{N,S}$ are replaced by $\xi'_{N,S} = c\xi_{N,S}$. The correction factor *c* is close to unity in our films and the effect on the critical temperature is small.
- ¹⁵O. Entin-Wohlman and S. Alexander, *J. Low Temp. Phys.* **24**, 229 (1976).
- ¹⁶G. Deutscher, O. Entin-Wohlman, and Z. Ovadyahu, *Phys. Rev. B* **14**, 1002 (1976).
- ¹⁷N. W. Ashcroft, and N. D. Mermin, *Solid State Physics* (HRW, Hong Kong, 1987); C. M. Soukoulis and D. A. Papaconstantopoulos, *Phys. Rev. B* **26**, 3673 (1982).
- ¹⁸A. F. Mayadas, R. B. Laibowitz, and J. J. Cuomo, *J. Appl. Phys.* **43**, 1287 (1972).
- ¹⁹A. Serfaty, J. Aponte, and M. Octavio, *J. Low Temp. Phys.* **1/2**, 23 (1986).
- ²⁰T. Kawakami, and H. Takanayagi, *Appl. Phys. Lett.* **46**, 92 (1985).
- ²¹D. Fenner, D. K. Biegelsen, and R. D. Bringans, *J. Appl. Phys.* **66**, 419 (1989); S. S. Iyer, M. Arienzo, and E. de Fresart, *Appl. Phys. Lett.* **57**, 893 (1990). Both articles contain an extensive list of references to earlier work on this subject.
- ²²S. R. Kasi *et al.*, *Appl. Phys. Lett.* **59**, 108 (1991).
- ²³A. Ikitoshi and Y. Shiraki, *J. Electrochem. Soc.* **133**, 666 (1986).
- ²⁴A. W. Kleinsasser *et al.*, *Appl. Phys. Lett.* **49**, 1741 (1986).
- ²⁵S. J. Park, and T. H. Geballe, *Physica B* **135**, 108 (1985).
- ²⁶E. T. Swartz, *Rev. Sci. Instrum.* **57**, 2848 (1986).
- ²⁷S. R. Mahamuni, D. T. Abell, and D. Williams, *Solid State Commun.* **68**, 145 (1988).
- ²⁸J. Y. Cheng and L. J. Chen, *Appl. Phys. Lett.* **58**, 45 (1991).
- ²⁹S. A. Wolf *et al.*, *J. Vac. Sci. Technol. A* **4**, 524 (1986); S. A. Wolf, J. J. Kennedy, and M. Nisenoff, *ibid.* **13**, 145 (1976).
- ³⁰M. Yu Kupriyanov and V. F. Lukichev, *Zh. Eksp. Teor. Fiz.* **94**, 139 (1988) [*Sov. Phys. JETP* **67**, 1163 (1988)].
- ³¹M. G. Kussianov, *Pis'ma Zh. Eksp. Teor. Fiz.* **53**, 554 (1991) [*JETP Lett.* **53**, 579 (1991)].
- ³²A. A. Golubov, M. Yu. Kupriyanov, V. F. Lukichev, and A. A. Orlikovskii, *Sov. Microelectron.* **12**, 355 (1983).
- ³³A. A. Golubov and M. Yu. Kupriyanov, *Phys. Lett. A* **154**, 181 (1991).
- ³⁴M. Yu. Kupriyanov and K. K. Likharev, *IEEE Trans. Magn.* **27**, 2460 (1991).